Structural and optical properties of chromium-doped hexagonal barium titanate ceramics

2008 J. Phys.: Condens. Matter 20 085206

(http://iopscience.iop.org/0953-8984/20/8/085206)

J. Phys.: Condens. Matter **20** (2008) 085206 (8pp) doi:10.1088/0953-8984/20/8/085206

Structural and optical properties of chromium-doped hexagonal barium titanate ceramics

H T Langhammer[1,4], T Müller[2], R Böttcher[3] and H-P Abicht[2]

[1] Physikalisches Institut, Martin-Luther-Universität Halle-Wittenberg, Friedemann-Bach-Platz 6, D-06108 Halle, Germany
[2] Chemisches Institut, Martin-Luther-Universität Halle-Wittenberg, Kurt-Mothes-Straße 2, D-06120 Halle, Germany
[3] Fakultät für Physik und Geowissenschaften, Universität Leipzig, Linnéstraße 5, D-04103 Leipzig, Germany

E-mail: hans.langhammer@physik.uni-halle.de, thomas.mueller@chemie.uni-halle.de, boettch@physik.uni-leipzig.de and hans-peter.abicht@chemie.uni-halle.de

Received 1 November 2007, in final form 17 December 2007
Published 1 February 2008
Online at stacks.iop.org/JPhysCM/20/085206

Abstract

The influence of chromium on the crystallographic phase and the microstructure of ceramics with the nominal composition $BaTiO_3 + 0.04BaO + xCr_2O_3$ ($0 \leqslant x \leqslant 0.025$) was investigated by systematic studies of x-ray diffraction (XRD) and electron paramagnetic resonance (EPR). At Cr concentrations $\leqslant 0.1$ mol% a hexagonal phase appears (room temperature). For nominal concentrations $\geqslant 1.0$ mol% the material is 100% hexagonal and its microstructure exhibits exaggerated, plate-like grains with a mean grain size $\geqslant 100$ μm (sintering temperature 1400 °C). In the hexagonal phase the EPR-active Cr_{Ti}^{3+} ions substitute both for Ti(1) (corner-sharing octahedron) and Ti(2) (face-sharing octahedron) sites. In air-sintered ceramics chromium is incorporated with valence states 3+ and 4+, whereas for reduced samples the valence state 3+ predominates. Optical transmission both of air-sintered and reduced samples doped with nominally 5.0 mol% Cr was measured in the visible light region. The absorption spectra exhibit distinct absorption bands. Their assignment to chromium defects with different valence states is discussed. The Jahn–Teller distortion caused by the electron configuration d^2 (Cr_{Ti}^{4+}) is proposed as the driving force for the high-temperature phase transition cubic → hexagonal.

1. Introduction

Barium titanate ceramics represents a material system of fundamental importance for a wide range of technical applications. Although there were, depending on temperature, five different phases observed, the focus of research was on the cubic and tetragonal phase, respectively, which transform into each other at the paraelectric–ferroelectric phase transition temperature near 125 °C. Much less information is available about the hexagonal high-temperature phase, which is stable at temperatures >1430 °C [1] as far as undoped, air-sintered material is concerned. The stability range of the hexagonal phase can be extended to room temperature both by firing in reducing atmospheres [2, 3] and by doping with some acceptor-type 3d transition elements like Mn, Fe or Ni [2, 4].

Recently, Jahn–Teller distortion was proposed to be the common driving force for the cubic–hexagonal transition [4]. The distortion is caused by Ti_{Ti}^{3+} ions in the undoped material or by Mn_{Ti}^{3+} and Cu_{Ti}^{2+}. Systematic investigations of manganese-doped [4] and copper-doped [5] barium titanate support the 'Jahn–Teller hypothesis'. Thus, it should also be tested with other Jahn–Teller active 3d transition ions like Cr_{Ti}^{4+}, in which the electron configuration d^2 (single electron term t_{2g}) causes the Jahn–Teller effect (JTE). However, to our knowledge, little is known about the influence of chromium on the stabilization of hexagonal barium titanate (h-BT) at room temperature, which is the prototype phase of the 6H stacking phase series of

[4] Author to whom any correspondence should be addressed.

barium titanate. In this series the high-temperature hexagonal phase (space group $P6_3/mmc$) transforms at about −50 °C into a orthorhombic phase ($C222_1$), which finally transforms at about −199 °C into the ferroelectric, monoclinic phase ($P2_1$) [6, 7].

Rather few investigations are known concerning the chromium impurity in $BaTiO_3$. Because of the rather large difference of the effective ionic radii between Ba^{2+} and Ti^{4+}, the incorporation of tri- or higher valent Cr on Ti sites is very probable, which has been supported by EPR investigations [8]. Hagemann and Ihrig [9] investigated Cr-doped $BaTiO_3$ up to 2 mol% Cr among other methods by measurement of the magnetic susceptibility. They determined the valence state of Cr_{Ti} in dependence on the oxygen partial pressure of the annealing atmosphere as 4+ (⩾0.2 bar, air or oxygen) or 3+ (10^{-22} bar, hydrogen). Due to the rather high Sr concentration of 1.7 mol% [10], their samples remained in the 3C stacking structure [11]. Among the investigations by electron paramagnetic resonance (EPR), see e.g. [8, 12, 13], Müller *et al* [8] investigated the Cr_{Ti}^{3+} defect in the 3C stacking series of $BaTiO_3$. Böttcher *et al* [13] extended the EPR investigations of Cr_{Ti}^{3+} for the phases with 6H stacking at a Cr concentration of 2.0 mol%. Only a little is known about optical investigations which can give additional information on the defect properties. The few studies were stimulated by the fact that Cr-doped $BaTiO_3$ is a potential photorefractive material [14]. Hatchcock *et al* [15] determined the optical absorption coefficients of an as-grown, electrically poled $BaTiO_3$ single crystal doped with 20 ppm Cr for both polarizations (electric field parallel and perpendicular to the *c* axis) in the visible light region. They found a distinct anisotropy of the absorption and a shift of the fundamental absorption edge to lower energies compared with nominally undoped material (≈3.0 eV), which gives the crystal a reddish colour. Eden *et al* [16] investigated optical absorption, photoluminescence and luminescence excitation of as-grown single crystals doped with 100 ppm (red tinted) and 1000 ppm (green tinted), respectively, in the visible light and near infrared region. They assumed Cr^{6+} transitions to be connected with the shift of the absorption edge, which increases with higher Cr content. Mazur [17] measured the optical absorption of three single crystals doped with 50, 100, and 500 ppm Cr, respectively, which were annealed in oxidizing or reducing atmosphere in the visible light region. In this work several Cr_{Ti} defects were identified by absorption and EPR measurements applying light induced charge transfer. Their valence states were determined as 4+ and 5+ (oxidized samples) and 3+ and 2+ (reduced samples), respectively.

Thus, the aim of this paper is the systematic investigation of the influence of Cr doping on the crystallographic structure of $BaTiO_3$ and, furthermore, of the properties of the Cr_{Ti} defects in hexagonal surrounding. To assist the desired Cr incorporation on Ti sites, a slight Ba excess of the samples was maintained. X-ray diffraction (XRD) was used to investigate the global crystal structure of the specimens. The former EPR investigation of Cr_{Ti}^{3+} in h-BT [13] was extended to the whole doping range up to 2 mol%, determining quantitative data of the Cr_{Ti}^{3+} concentrations. Optical absorption in the visible light region was measured to get additional information about the Cr defect. Compared to the known investigations of optical absorption [15–17], the specimens investigated had at least one order higher doping concentration.

2. Experimental details

Ceramic powders with the nominal composition $BaTiO_3 + 0.04BaO + x/2\ Cr_2O_3$ ($0 \leqslant x \leqslant 0.05$) were prepared by the conventional mixed-oxide powder technique. After mixing (agate balls, water) and calcining (1100 °C, 2 h) of $BaCO_3$ (Solvay, VL600, <0.1 mol% Sr) and TiO_2 (Merck, no 808), Cr_2O_3 (Merck, p.a.) was added to the $BaTiO_3$ powder. Then it was fine-milled (agate balls, 2-propanole) and densified to discs with a diameter of 6 mm and a height of nearly 3 mm. The samples were sintered in air at temperatures of 1350 and 1400 °C for 1 h (heating rate 10 K min^{-1}). Samples sintered at 1400 °C were additionally annealed under oxidizing (pure oxygen) and reducing (1:1 mixture of hydrogen and argon) conditions in a gas stream of 40 ml min^{-1} (normal pressure) at 1200 °C for 2 h. The microstructure of polished and chemically etched specimens was examined by optical microscopy and scanning electron microscopy (SEM). To determine the Cr distribution in the grains and intergranular regions, wavelength-dispersive x-ray electron probe microanalysis (WDX-EPMA) (model CAMEBAX, Cameca, France) was carried out. The overall phase composition was determined quantitatively, analysing the XRD intensity ratios (peak heights) $(111)_{tetragonal}/(103)_{hexagonal}$ and $(200)_{tetragonal}/(103)_{hexagonal}$ calibrated by well defined mixtures of pure tetragonal and hexagonal barium titanate powders (STADI MP diffractometer, STOE, Germany). EPR measurements of finely pulverized samples were carried out in the X band (9 GHz) with a Varian E 112 spectrometer and in the Q band (34 GHz) with a Bruker EMX device. More details of the measuring procedure are described in [13]. Room temperature optical absorption measurements in the 350–800 nm region were performed using a microscope photometer, model MPM 800D/UV (Carl Zeiss, Germany). To achieve sufficient optical transmission the samples (mounted on a microscope slide) had to be thinned down to a thickness below 30 μm by mechanical grinding and polishing.

3. Results

3.1. X-ray diffraction

Figure 1 shows the percentage of tetragonal phase as a function of the nominal Cr concentration. In the whole Cr-doping range investigated, exclusively tetragonal and hexagonal phases were found within the detection limit of roughly 5 wt%. Thus, the remaining percentage corresponds to the hexagonal phase. For a sintering temperature of 1400 °C h-BT occurs above a minimum Cr concentration of less than 0.1 mol%. Since the used TiO_2 powder already contains small amounts of Cr impurities, the threshold value could not be determined more precisely. But a sample from highly pure, commercial $BaTiO_3$ powder (Transelco, no 219-9) with

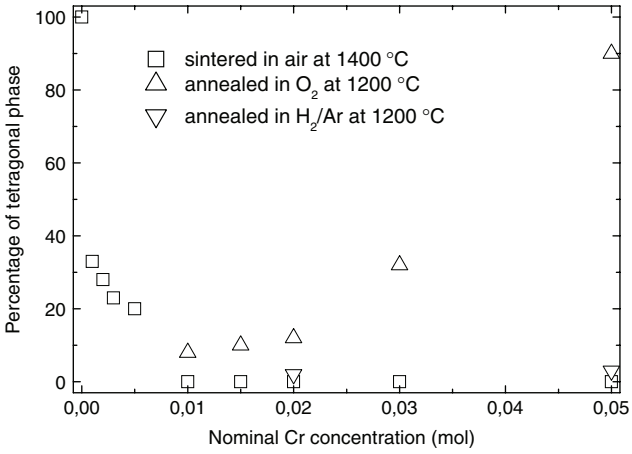

Figure 1. Percentage of tetragonal phase of as-sintered, oxidized and reduced Cr-doped $BaTiO_3$ at room temperature as a function of the nominal Cr concentration.

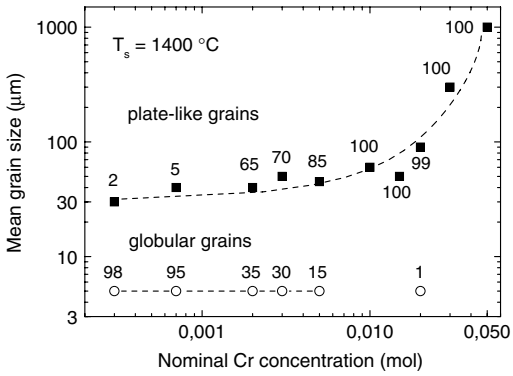

Figure 2. Average grain sizes of $BaTiO_3$ ceramics as a function of the nominal Cr concentration. Numbers at data symbols denote the portions of grain fractions, roughly estimated manually from the areas in a two-dimensional sample-cut.

Ba:Ti = 1.04 (sintered at 1400 °C) was completely tetragonal. At Cr concentrations $\geqslant$1.0 mol% the samples are completely hexagonal. For a sintering temperature of 1350 °C (not shown in figure 1) the threshold concentration to produce h-BT amounts to nearly 0.4 mol% Cr and at 5.0 mol% the hexagonal portion reaches 90%.

The 100% hexagonal samples were additionally annealed under oxidizing and reducing conditions, respectively. The phase composition of those samples is also shown in figure 1. Whereas the reducing treatment decreases the percentage of hexagonal phase only a little, the oxidizing treatment considerably retransforms the samples into the tetragonal phase (room temperature). The percentage of retransformed phase increases with increasing Cr content up to 90% at 5 mol% nominal Cr content.

3.2. Microstructure and solubility of chromium in $BaTiO_3$

The dependence of the phase composition on the doping level is reflected very well by the development of the microstructure (figure 2). Since the Ba-excess of the samples safely prevents the occurrence of a Ti-rich liquid phase, the undoped material exhibits normal grain growth with globular grains of about 5 μm in size. At very low Cr concentrations of $\leqslant$0.1 mol% the microstructure becomes bimodal. One fraction of grains corresponds to these small globular grains, of which the percentage decreases with increasing Cr content and vanishes when the samples become completely hexagonal. The other fraction exhibits exaggerated growth, plate-like shaped grains of which the percentage increases in accordance with the amount of hexagonal phase. This grain fraction is typical for h-BT [3–5]. With increasing percentage of the plate-like grains, they touch each other during grain growth and the distinct plate-like shape vanishes gradually. Their grain size increases with increasing Cr content and reaches more than 1000 μm at a nominal concentration of 5.0 mol%. The obviously liquid phase-assisted, exaggerated grain growth is probably caused by a Cr-containing eutectic with unknown composition.

Because of the limited solubility of many dopants, the amount of Cr incorporated into the grown grains of $BaTiO_3$ was quantitatively determined by WDX-EPMA for a nominal Cr content of 1.5 and 5.0 mol%, respectively. Figure 3 shows the measured Cr concentration along a line over a sample with 5.0 mol% Cr. Considerable amounts of Cr are segregated at grain boundaries, triple points and intragranular pores. Only about 2.8 mol% Cr (56% of the nominal content) is incorporated into the crystal structure of the grains. For a nominal concentration of 1.5 mol% Cr, about 73% is incorporated.

3.3. Electron paramagnetic resonance

Typical data of a nominally 2.0 mol% Cr-doped sample are shown in figure 4 as the first derivative of the absorption EPR spectrum in the X band measured at room temperature [13]. The spectrum can be divided into three partial spectra labelled by T1, H1 and H2. They are assigned to $^{50,52,54}Cr^{3+}$ ions incorporated at different Ti sites in tetragonal (T1) and hexagonal (H1, H2) $BaTiO_3$. The spectra present mainly fine structure (fs) peaks, of which the parameters are determined by axial fs parameters D. Weak hyperfine transition peaks arising from $^{53}Cr^{3+}$ (natural abundance 9.5%, nuclear spin = 3/2) could only be detected in the Q band T1 spectrum. This spectrum corresponds very well to single crystal results of Müller *et al* [8]. The assignment of the spectra H1 and H2 was done by analysis of the fs peaks and their dependences on frequency and measuring temperature as well as by the investigation of small hexagonal single crystals; for details see Böttcher *et al* [13]. The spectra H1 and H2 correspond to Cr^{3+} incorporated at both chemically non-equivalent Ti sites Ti(1) and Ti(2) of the hexagonal lattice. Whereas the Ti(1) site belongs to the exclusively corner-sharing oxygen octahedra, which are the only structural units of the 3C stacking phase series of $BaTiO_3$, the Ti(2) site is inside the face-sharing octahedra, constituting two-thirds of the structural units of the 6H stacking phase series. This is in contrast to Mn-doped hexagonal $BaTiO_3$, in which the Mn^{4+} ion only substitutes at the Ti(1) lattice site [18]. Furthermore, it was found that

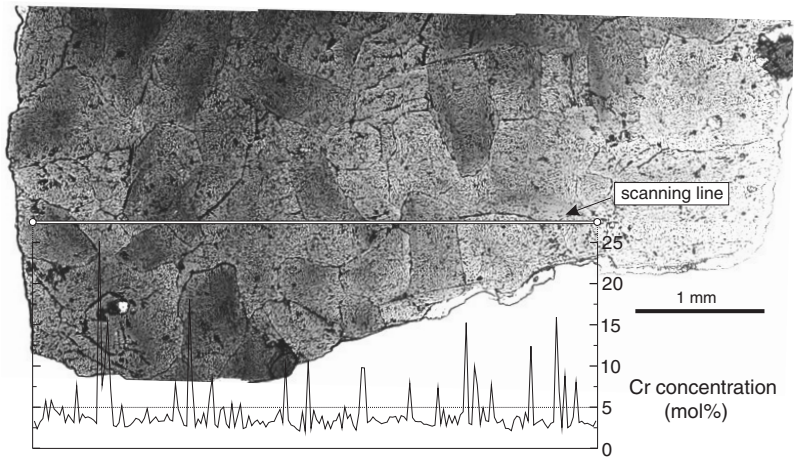

Figure 3. Optical micrograph (transmitted light) of a thinned sample (≈14 μm) of $BaTiO_3$ doped with nominal 5.0 mol% Cr. The inset shows the Cr concentrations along a scanning line measured by EPMA.

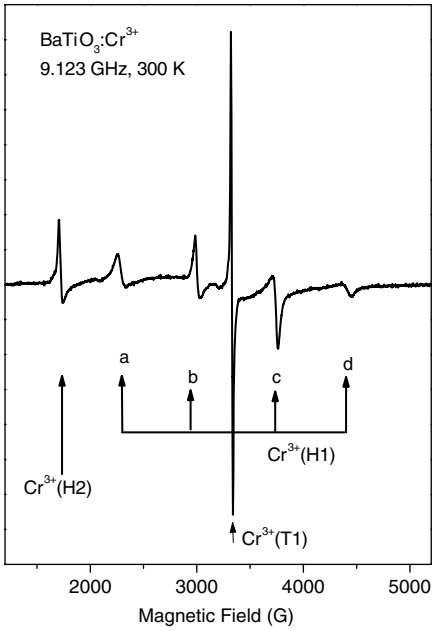

Figure 4. Room temperature EPR spectrum of $BaTiO_3$ doped with nominal 2.0 mol% Cr, measured in the X band (from [13]). The labels T1, H1, and H2 correspond to different partial spectra explained in the text; letters a–d label the different fine structure peaks of partial spectrum H1.

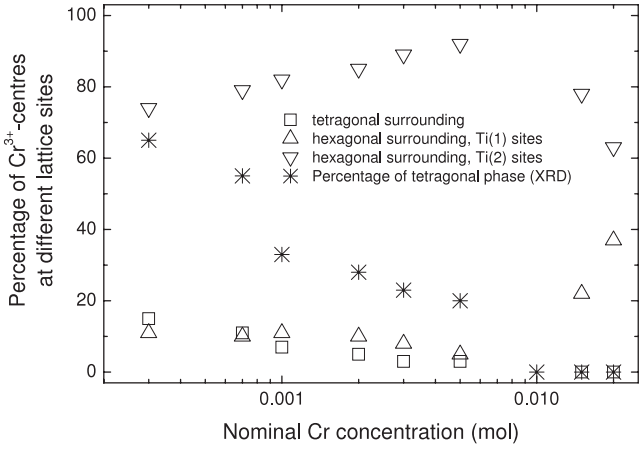

Figure 5. Percentage of Cr^{3+} centres at different lattice sites of as-sintered Cr-doped $BaTiO_3$ derived from EPR together with the percentage of tetragonal phase (XRD) as a function of the nominal Cr concentration.

both $Cr^{3+}_{Ti(1)}$ and $Cr^{3+}_{Ti(2)}$ do not form associates with oxygen vacancies, which must be present in the lattice due to charge balance, but they are encircled by six oxygen ions [13].

Since the parameters of the EPR spectra could be determined with high accuracy by simultaneous simulating the multi-frequency spectra [13], quantitative analysis of the Cr^{3+} concentrations was possible (double integration of the simulated Q-band spectra). The results are shown in figure 5. Note that the percentages of Cr^{3+} concentration are not related to the total amount of Cr incorporated into the grains but give only the ratio between the three different incorporation variants. Also note that the XRD data reflect the global phase composition whereas EPR probes the local environment of the Cr^{3+} impurity. The EPR-determined concentrations of Cr^{3+} in tetragonal surroundings of the samples with coexistence of both phases are systematically lower than the XRD data. Whereas at lower Cr concentrations only minor amounts of Cr prefer the incorporation into the exclusively corner-sharing octahedra, their percentage increases significantly in the large-grown grains of the 100% hexagonal samples.

The annealed samples were also investigated by EPR. The reduced samples exhibit all three spectra T1, H1 and H2 found in as-sintered specimens. Their Cr^{3+} concentrations are generally increased, causing a line-broadening of all peaks. Additionally, a new broad line occurred with an electronic g-factor of 1.974 and a frequency-independent linewidth of 240 G, which could be caused by Cr^{3+} in eluted secondary phase (as oxide or Cr clustering). Contrary to these findings, the oxidation process caused a nearly complete transformation of the hexagonal spectra H1, H2 into the tetragonal one (T1). Only a very weak H2 spectrum is detectable.

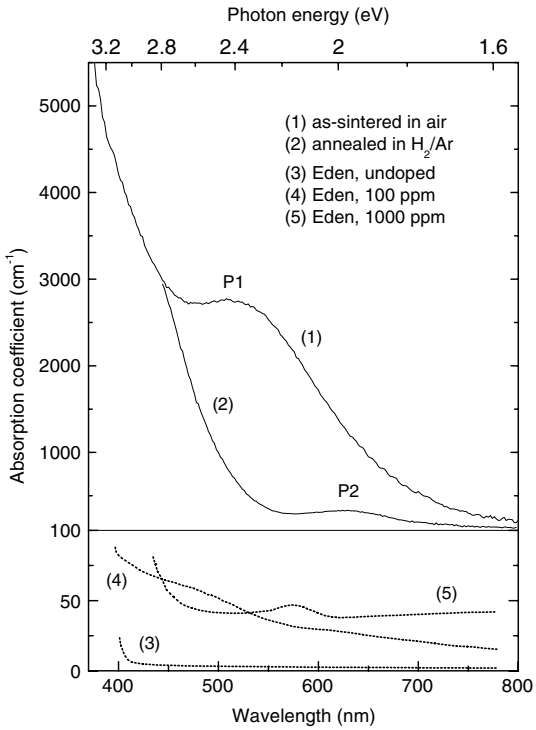

Figure 6. Absorption spectra (unpolarized light) of 5.0 mol% Cr-doped thinned $BaTiO_3$ ceramics, (1) as sintered in air, (2) annealed in H_2/Ar, and single crystal data from Eden *et al* [16], (3) undoped, (4) nominal 100 ppm Cr, (5) nominal 1000 ppm Cr. Note the different scales above and below 100 cm^{-1}.

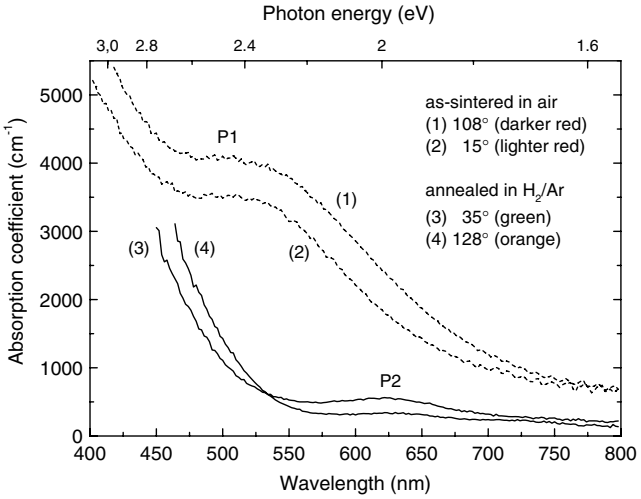

Figure 7. Absorption spectra (linearly polarized light) of 5.0 mol% Cr-doped $BaTiO_3$ ceramics. As-sintered sample, (1) 108°, (2) 15°; reduced sample, (3) 35°, (4) 128°. The given angles mean the direction of the electric field vector related to a fixed direction of the sample holder.

3.4. Optical absorption

Because of their polycrystalline, ceramic structure and their high absorption coefficient in the visible light region, '1 mm thick' samples are non-transparent and appear dark brown and changing to black, corresponding to a doping level of about 0.1 mol% up to 5 mol% chromium. If the specimens are thinned down below 50 μm, they gradually become translucent and exhibit a characteristic colour depending on the kind of the dopant and on its concentration. Optical transmission (T) measurements of thinned samples were performed with measuring areas of between 5×5 and 15×15 μm^2 to ensure that the light passes through a single crystalline, homogeneous, and pore-free part of a selected grain. Since no reflectivity (R) data were available, no correct absorption coefficients could be obtained by the formula (approximately valid for $R < 0.25$ and/or $\alpha d \geqslant 1$)

$$T = (1 - R)^2 e^{-\alpha d} \quad (1)$$

where α and d are the absorption coefficient and the sample thickness, respectively. Thus, the absorption coefficients of the spectra presented in figure 6 were calculated formally setting $R = 0$. The reflectivity of undoped $BaTiO_3$ single crystals varies continuously between 0.15 (800 nm) and 0.24 (400 nm) [19, 20], where the enlarged increase of R below 600 nm is caused by the fundamental transition near 400 nm. Hence, the error of the presented absorption data amounts to +230 cm^{-1} (800 nm) and +400 cm^{-1} (400 nm) for the as-sintered sample with $d = 14$ μm and +120 cm^{-1} (800 nm) and +200 cm^{-1} (400 nm) for the reduced sample with $d = 27$ μm, respectively, if we assume that the absorption processes of the Cr_{Ti} defect influence the reflectivity spectrum only slightly. Figure 6 shows the absorption coefficients of two specimens with a nominal Cr content of 5 mol% measured with unpolarized light. While the as-sintered sample exhibits a red or reddish-brown colour, the heavily reduced one is green, with some grains changing the colour to orange. The remarkable features of these spectra are the absorption bands P1 and P2 of the as-sintered and reduced sample, respectively, and the shift of the strong absorption edge to lower energies compared to undoped $BaTiO_3$ (also shown in figure 6). According to the discussion above, the quantitative error of the absorption coefficients could not significantly change these observed properties. The spectra of the two samples were also measured with linearly polarized light, shown in figure 7. Since the spatial orientation of the crystal axes of the grains investigated is unknown, the spectra were taken at directions of the electric field vector either where the integral transmission was minimal and maximal, respectively (as-sintered sample), or where the differences in colour were maximal (reduced sample). In both cases, the angle between these directions amounted to nearly the expected 90°, because h-BT is optically uniaxial with the hexagonal c-axis as the principal axis. For the as-sintered specimen both spectra are related to a roughly energy-independent different absorption coefficient, i.e. the reddish shade of the sample does not change. In the case of the reduced specimen, the different spectra exhibit different onset wavelengths of the strong absorption edge, and the change of the polarizing direction is accompanied by a gradual change of the specimen's shade between green and orange. On the other hand, the spectral position of the band P2 does not depend on the direction of polarization checked at several measuring points in different grains.

4. Discussion

4.1. Phase transformation

The dependences of overall phase composition and microstructure on the doping level are qualitatively in complete accordance with the results of manganese [4] and copper [5] doped barium titanate. Thus, chromium also stabilizes the 6H stacking series of $BaTiO_3$, which is hexagonal at room temperature. Compared to the dopants Mn and Cu, the chromium impurity exhibits both the lowest threshold concentration for occurrence of hexagonal phase of roughly 0.1–0.2 mol% (Mn: >0.5 mol%, Cu: >0.2 mol%) and the lowest necessary concentration to obtain complete h-BT of 1.0 mol% (Mn: 1.6 mol%, Cu: ≈2.0 mol%). These values are valid for sintering in air at 1400 °C and for a sufficiently low concentration of strontium below 0.1 mol% [11]. Hence, among the dopants Mn, Cu and Cr, the latter is the most effective one for stabilizing the hexagonal phase at room temperature, but it has the lowest solubility since it needs the highest excess of 4.0 mol% BaO for a sufficiently high incorporation into the $BaTiO_3$ lattice (Mn, no excess necessary; Cu, 3.0 mol%).

Two conditions are required for the high-temperature transformation of $BaTiO_3$ from its cubic into its hexagonal phase. First, a sufficiently high density of oxygen vacancies[5] $V_O^{\bullet\bullet}$ is necessary to change the stacking of the BaO_3 layers (the main constituents of the crystal structure of $BaTiO_3$) from 3C to 6H, which could proceed via reciprocal gliding of adjacent lattice planes [4]. Oxygen vacancies are caused by thermodynamic reasons (Schottky vacancies) and by charge compensation of the acceptor dopant (e.g. $Cr_{Ti}^{\prime(3+)}$). Thus, the temperature for the necessary minimum concentration $[V_O^{\bullet\bullet}]$ decreases with increasing doping level. Second, a driving force should act as the initiator of the phase transformation. As in the case of undoped, Mn-doped and Cu-doped $BaTiO_3$ [4, 5], we propose also for the Cr-doped material the influence of the Jahn–Teller distortion (see, e.g., [21]). For example, Cr_{Ti}^{4+} or Cr_{Ti}^{2+} with its d^2 or d^4 configuration causes a weak or strong JTE, respectively, in octahedral oxygen environment. Hence, the resulting local lattice distortion may initiate the phase transition. Thus the lower transition temperature of the doped material can be explained. The phase transition takes place, provided that the concentrations both of the oxygen vacancies *and* of the JTE active acceptor ions are high enough and the ionic mobilities are sufficiently high. However, in the initial stage of the phase transition of a polycrystalline material, only a few single crystallites (grains) transform, which results in a phase coexistence in certain ranges of doping level and sintering temperature, respectively. The different threshold concentrations for the occurrence of hexagonal phase could point to different concentrations of the JTE active ions Mn_{Ti}^{3+}, Cu_{Ti}^{2+} and Cr_{Ti}^{4+} in the temperature region of the phase transition cubic–hexagonal $\gtrsim$ 1300 °C.

The general restoration of the tetragonal phase by annealing in both oxidizing and reducing atmospheres can be understood by the fact that the 6H $BaTiO_3$ is not in the equilibrium state at room temperature, but is in a frozen state, since the gliding of the BaO_3 planes back to the 3C stacking is only possible at sufficiently high temperatures and time. The annealing in strongly reducing atmosphere causes remarkable concentrations of $Ti_{Ti}^{\prime(3+)}$ due to the charge compensation of the produced oxygen vacancies $V_O^{\bullet\bullet}$. The d^1 configuration of $Ti_{Ti}^{\prime(3+)}$ causes a weak JTE, which prevents for the most part the restoration of the tetragonal phase at the annealing temperature of 1200 °C, which can explain the drastic difference in the restoration behaviour of the annealing in oxidizing and reducing atmosphere. Mn-doped $BaTiO_3$ ceramics behave quite oppositely with respect to the amount of restored tetragonal phase depending on the annealing atmosphere [4]. The corresponding discussion in [4] shows that generally many more factors influence the real development of the crystal structure in dependence on doping level and thermodynamic parameters.

4.2. Chromium defect

The comparison of the EPR-derived total concentrations of Cr_{Ti}^{3+} [13] with the true chromium concentration in the grains (measured by EPMA) makes clear that only a part of the chromium in the $BaTiO_3$ lattice is in the valence state 3+. In air-sintered specimens the valence state 2+ is rather unlikely, which is confirmed by calculations of 3d electron energy levels and of the stability of Cr ions in $BaTiO_3$ [22, 23]. Since the EPR-active valence state 5+ was not detected (at room temperature), the highest oxidation state 6+ also seems to be unlikely. Hence, the remaining Cr should be in the EPR-silent state 4+. A rough estimation for a sample with nominal 2.0 mol% Cr resulted in 45% Cr_{Ti}^{3+} and 55% Cr_{Ti}^{4+}. This is not in complete accordance with Hagemann and Ihrig [9], who stated 4+ as the predominant valence state in air-sintered samples. The EPR data of the annealed specimens prove the expected change of the valence state to be nearly exclusive 4+ (oxidized samples) and predominant 3+ (reduced samples), respectively, though the highly reducing atmosphere could also cause some of the EPR-silent Cr_{Ti}^{2+}, asserted by Mazur [17] using measurements of optical absorption and EPR of single crystals and of the changes of the Cr charge states under illumination. Figure 8 shows again the absorption spectra of the ceramic specimens together with the spectra of an as-grown and a reduced Cr-doped single crystal published by Mazur and the absorption spectrum of an undoped single crystal published by Eden *et al* [16] in dependence on the photon energy. The nominal Cr content (in the melt) of the as-grown and reduced crystals amounted to 100 and 50 ppm, respectively, which corresponds to 0.045 and 0.022 mol% Cr or less, since probably less than half of the added Cr is incorporated into the crystal [16]. This explains the large differences in the absorption coefficients of the nominally 5.0 mol% (incorporated 2.8 mol%) Cr-doped ceramic samples and the single crystals. For the interpretation of the absorption spectra, Mazur assumed charge transfer (from valence band to defect) as well as intervalence (from defect to conduction band) excitations while neglecting crystal field transitions, since they are generally much weaker, being essentially forbidden

[5] Here and in the following the Kröger–Vink notation of point defects is used occasionally.

Table 1. Selected parameters of a two-peak Gaussian fitting of the absorption coefficient in dependence on photon energy of the ceramic samples.

	Absorption bands P1, P2		Strong absorption at higher energy	
Specimen	Central pos. (eV)	Strength (cm^{-1})	Central pos. (eV)	Strength (cm^{-1})
As-sintered	2.28	860	4.5	27 000
Reduced	1.97	57	3.0	2 900

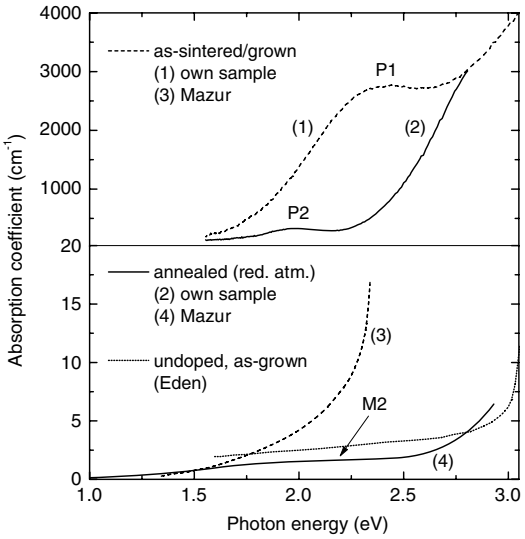

Figure 8. Absorption spectra (unpolarized light) of 5.0 mol% Cr-doped $BaTiO_3$ ceramics (redrawn data from figure 6), (1) as-sintered, (2) reduced, and of different single crystals, from Mazur [17] (3) 100 ppm Cr, as-grown, (4) 50 ppm Cr, reduced, and from Eden [16] undoped, as-grown. Note the different scales above and below 20 cm^{-1}.

transitions. For the as-grown crystal, he attributed the strong absorption onset at energies $>$ 2.3 eV to an excitation of a valence band electron to Cr^{4+}, forming Cr^{3+}. For the reduced crystal, he stated Cr^{2+} to be responsible for the broad absorption band M2 near 2.0 eV, caused by an intervalence transition, and the excitation of a valence band electron to Cr^{3+}, leading to Cr^{2+}, for the strong absorption onset at energies $>$ 2.5 eV.

Despite the much higher defect concentrations of our ceramic specimens, their absorption spectra are qualitatively similar to Mazur's data. The reduced samples are more transparent than the as-grown/as-sintered, i.e. they have higher onset energies of strong absorption. Furthermore, the bands P2 and M2 of the reduced specimens can be related to each other and the strong increase of absorption of the as-grown single crystal near 2.3 eV could be related to the absorption band P1 of the as-sintered ceramic. Thus, we could adopt Mazur's assignment to the Cr defects for the ceramic specimens. Since obviously in both ceramic samples at least two absorption processes overlap, we tried to disentangle them by fitting with two Gaussian functions. The resulting parameters are shown in table 1. Despite the different peak positions of the strong absorption bands of both samples, their 'onset points' are rather similar. Thus, additionally taking into account that both ceramic specimens contain considerable amounts of Cr^{3+}, we propose that the increasing strong absorption at 2.3 eV and 2.7 eV of the reduced and as-sintered sample, respectively, originates in both cases from charge transfer excitations involving Cr^{3+}.[6] Then, in accordance with the interpretation by Mazur, the band P1 must be related to Cr^{4+} (charge transfer, leading to Cr^{3+}), consistent with its vanishing after a reducing annealing.

For the weak absorption band P2 of the reduced sample we also could follow Mazur's proposal as being related to intervalence excitations of Cr^{2+}. On the other hand, since its strength is only about 1/15 of the strength of P1 (see table 1), crystal field transitions of Cr^{3+} or Cr^{2+} should not completely excluded. Since the absorption spectra of the 3C and 6H stacking modification of undoped $BaTiO_3$ around the fundamental absorption edge are very similar in a broad temperature range (room temperature to 620 K) [24] the comparability of our hexagonal samples with Mazur's tetragonal (at room temperature) single crystals should be ensured.

5. Conclusions

Cr-doped $BaTiO_3$ ceramics sintered at 1400 °C in air change gradually their room temperature crystallographic structure from tetragonal to hexagonal, beginning with Cr concentrations of about 0.1 mol%. EPR measurements revealed that in both phases Cr^{3+} is incorporated at Ti sites. In the hexagonal lattice both chemically non-equivalent sites Ti(1) and Ti(2) are occupied. Whereas at lower Cr concentrations the substitution at Ti(2) sites dominates, the concentration of $Cr^{3+}_{Ti(1)}$ increases with increasing doping level after the material becomes completely hexagonal. In all cases the Cr^{3+} ions are isolated defects and the compensating oxygen vacancies are localized outside the surrounding oxygen octahedron. At room temperature, chromium coexists in the valence states 3+ and 4+ in as-sintered samples. Samples doped with nominal 2.0 mol% Cr exhibit similar concentrations of both valence states. An annealing in oxygen retransforms the samples from the 6H back to the 3C stacking structure. We suggest that the cubic–hexagonal phase transformation of Cr-doped $BaTiO_3$ is driven by a Jahn–Teller distortion caused by Cr^{4+}_{Ti}. Optical absorption spectra of nominally 5.0 mol% Cr-doped specimens exhibit distinct absorption bands in the visible light region. The following causes of these bands are proposed. The strong absorption bands immediately below the fundamental absorption of both the as-sintered (air) and reduced sample are due to charge

[6] The onset point of the absorption band of the as-sintered specimen is hidden by the overlap with band P1.

transfer excitations of Cr^{3+} to Cr^{2+}. The lower energetic absorption bands of both samples are explained by charge transfer (Cr^{4+}/Cr^{3+}, as-sintered specimen) and intervalence transition (Cr^{2+}/Cr^{3+}, reduced specimen), not excluding crystal field transitions of Cr^{2+} or Cr^{3+} for the latter.

Acknowledgments

The authors thank Klaus-Jürgen Berg for providing the optical laboratory and Christine Seidel (Physical Institute, Faculty for Chemistry and Physics, Martin-Luther-Universität Halle-Wittenberg) for the measurement of the optical absorption, including the careful preparation of thinned ceramic samples. Last but not least, the authors thank Professor O F Schirmer (Universität Osnabrück) for very valuable discussion related to the interpretation of the optical absorption spectra.

References

[1] Kirby K W and Wechsler B A 1991 *J. Am. Ceram. Soc.* **74** 1841
[2] Glaister R M and Kay H F 1960 *Proc. Phys. Soc.* **76** 763
[3] Kolar D, Kunaver U and Rečnik A 1998 *Phys. Status Solidi* a **166** 219
[4] Langhammer H T, Müller T, Felgner K-H and Abicht H-P 2000 *J. Am. Ceram. Soc.* **83** 605
[5] Langhammer H T, Müller T, Böttcher R and Abicht H-P 2003 *Solid State Sci.* **5** 965
[6] Sawaguchi E, Akishige Y, Yamamoto T and Nakahara J 1989 *Ferroelectrics* **95** 29
[7] Noda Y, Akiyama K, Shobu T, Kuroiwa Y and Yamaguchi H 1999 *Japan. J. Appl. Phys. Suppl.* **38-1** 73
[8] Müller K A, Berlinger W and Albers J 1985 *Phys. Rev.* B **32** 5837
[9] Hagemann H-J and Ihrig H 1979 *Phys. Rev.* B **20** 3871
[10] Hagemann H-J 1980 Akzeptorionen in $BaTiO_3$ und $SrTiO_3$ und ihre Auswirkung auf die Eigenschaften auf Titanatkeramiken *PhD Thesis* RWTH Aachen, Germany, p 30
[11] Langhammer H T, Müller T, Felgner K-H and Abicht H-P 2000 *Mater. Lett.* **42** 21
[12] Schwarz R N and Wechsler B A 1993 *Phys. Rev.* B **48** 7057
[13] Böttcher R, Erdem E, Langhammer H T, Müller T and Abicht H-P 2005 *J. Phys.: Condens. Matter* **17** 2763
[14] Schirmer O F 1999 *Radiat. Eff. Defects Solids* **149** 1
Briat B, Grachev V G, Malovichko G I, Schirmer O F and Wöhlecke M 2007 *Photorefractive Materials and Their Applications* vol 2, ed P Günter and J P Huignard (Berlin: Springer) pp 9–49
[15] Hatchcock R S, Temple D A and Warde C 1987 *IEEE J. Quantum Electron.* **23** 2122
[16] Eden S, Kapphan S, Hesse H, Trepakov V, Vikhnin V, Gregora I, Jastrabik L and Seglins J 1998 *J. Phys.: Condens. Matter* **10** 10775
[17] Mazur A 1999 Light-induced charge transfer processes between defects in oxide perovskites *PhD Thesis* Universität Osnabrück, Germany (Aachen: Shaker)
[18] Böttcher R, Langhammer H T, Müller T and Abicht H-P 2005 *J. Phys.: Condens. Matter* **17** 4925
[19] Cardona M 1965 *Phys. Rev.* **140** A651
[20] Gerthsen P, Groth R and Härdtl K H 1965 *Phys. Status Solidi* **11** 303
[21] Bersuker I B 1975 *Coord. Chem. Rev.* **14** 357
[22] Moretti P and Michel-Calendini F M 1986 *Phys. Rev.* B **36** 3522
[23] Moretti P and Michel-Calendini F M 1988 *J. Opt. Soc. Am.* B **5** 1697
[24] Akishige Y 1995 *J. Phys. Soc. Japan* **64** 4033